

Krzysztof MAGNUCKI ¹

Bending of a five-layered composite beam with consideration of two analytical models

Received 17 October 2023, Revised 4 February 2024, Accepted 15 February 2024, Published online 28 March 2024

Keywords: composite beam, zig-zag theory, nonlinear shear deformation theory

The subject of the work is a five-layered composite beam with clamped ends subjected to a uniformly distributed load along its length. Two analytical models of this beam are developed with consideration of the shear effect. The first model is formulated on the basis of the classical zig-zag theory. Whereas, the second model is developed using an individual nonlinear shear deformation theory with consideration of the classical shear stress formula (called Zhuravsky shear stress). The system of two differential equations of equilibrium for each beam model is obtained based on the principle of stationary total potential energy. These systems of equations are exactly analytically solved. The shear effect function and the maximum deflection are determined for each of these two beam models. Detailed calculations are carried out for exemplary beams of selected dimensionless sizes and material constants. The main goal of the research is to develop two analytical models of this beam, determine the shear effect function, the shear coefficient, and the maximum deflection in the elastic range for each model, as well as to perform a comparative analysis.

1. Introduction

Sandwich structures are intensively refined and used in many constructions in the 21st century. Carrera [1] presented a very insightful historical review of the Zig-Zag theories used in the analysis of multilayer structures, including 138 references. On the basis of this review, he distinguished three multilayer theories named: Lekhnicki (LMT) initiated in 1935, Ambartsumian (AMT) initiated in 1958 and Reissner (RMT) generalized in 1984. Huang [2] developed an analytical model of a five-layer beam with two facings, two adhesive layers, and a core, taking into

✉ Krzysztof MAGNUCKI, e-mail: krzysztof.magnucki@pit.lukasiewicz.gov.pl

¹Łukasiewicz Research Network, Poznan Institute of Technology, Poznan, Poland



account the conditions of displacement continuity. Detailed calculations of an exemplary beam subjected to three-point bending were performed analytically, FEM numerically and taking into account the theory proposed by Allen (1969). Pollien et al. [3] presented a process for producing functionally graded porous structures. The produced five- and seven-layer beam samples were subjected to three-point bending on the test stand. Hu et al. [4] conducted an analysis and evaluation of various theories used in the modelling of layered composites. They considered the following theories: classical laminate (CLT), first-order (FSDT) and high-order (HOT) shear deformations, zig-zag, and a proposed unified kinematic formulation. Comparative tests of exemplary beams with solution by the finite element method were carried out. Reddy [5] characterized Euler-Bernoulli, Timoshenko beam theories, classical plate theory, and first-order shear deformation plate theory, and then reformulated these theories taking into account the non-local differential constitutive relation of Eringen and the von Kármán non-linear strain. Chakrabarti et al. [6] developed a new finite element model taking into account the higher-order zig-zag theory (HOZT). Numerical calculations of exemplary composite beams with different properties were performed in order to demonstrate the accuracy of the developed element. Carrera et al. [7] presented many refined beam theories that they developed taking into account Taylor polynomials, trigonometric series, exponential, hyperbolic, and zig-zag functions. The results of exemplary calculations of the described models are compared in terms of displacements, stresses, and degrees of freedom. Magnucki et al. [8] developed an analytical model of a five-layer sandwich beam with two thin layers of glue and analyzed its three-point bending. The results of the analytical tests of the sample beams were compared with the results of the FEM numerical tests. Smyczyński and Magnucka-Blandzi [9] analyzed the problem of dynamic stability of a simply supported five-layer sandwich beam. On the basis of Hamilton's principle, a system of three differential equations of motion was determined. The unstable regions and equilibrium paths were determined for the example beams.

Paczos et al. [10] studied five-layered trapezoidal beams in analytical, numerical (FEM), and experimental approaches. An analysis of the sensitivity of selected geometrical parameters to their stiffness was carried out. Icardi and Sola [11] analyzed the bending of sandwich beams and rectangular slabs with different boundary conditions using the equivalent single-layer zig-zag model. Magnucka-Blandzi et al. [12] developed an analytical model of the untypical orthotropic seven-layered beam and determined the critical load and the natural frequency. Detailed buckling and vibration analysis for the example beams was performed analytically and numerically by FEM. Vo et al. [13] analyzed the bending of composite and sandwich beams, taking into account the developed two-node beam elements with six degrees of freedom. The influence of the position of the fibers on displacements and stresses was investigated. Smyczyński and Magnucka-Blandzi [14] studied analytically, numerically FEM, and experimentally a five-layer beam subjected to three-point bending. Two analytical models of the beam were developed, taking into

account the “broken line” theory and the non-linear theory. Detailed calculations were carried out exemplary beams.

Zhai et al. [15] analyzed the natural vibrations of two five-layer composite sandwich plates with double-layer viscoelastic cores, taking into account the first-order shear deformation theory. Pei et al. [16] presented a modified higher-order shear deformation theory for FG beams and analytical bending studies of these simply supported and cantilevered beams. Wang et al. [17] analytically studied the wave propagation problem in porous beams with consideration of the Euler-Bernoulli and Timoshenko beam theories. Wang et al. [18] numerically and experimentally studied a laminated composite beam composed of 20 aluminium layers subjected to impact loads. Garg and Chalak [19] developed a new higher-order zig-zag theory for the analysis of laminated sandwich beams, which was included in the sample studies using a three-node one-dimensional finite element with eight degrees of freedom in a node. Magnucki et al. [20] analyzed the problems of bending, buckling, and free vibration of a simply supported sandwich beam, taking into account three models: classical “broken line”, nonlinear shear effect in the core, and nonlinear shear effect in the faces and the core. Magnucki [21] developed an individual non-linear shear deformation theory of beams and studied in detail beams with the homogeneous, sandwich and variable mechanical properties of beams subjected to three-point bending. Magnucki and Magnucka-Blandzi [22] presented in detail a refined shear deformation theory of an asymmetric sandwich beam taking into account the classical shear stress formula.

The subject of the study is a clamped five-layered composite beam of length L , width b , and total depth h under a uniformly distributed load of intensity q (Fig. 1). The main goal of this paper is to elaborate two analytical models of this beam and to conduct a comparative analysis of the calculation results obtained from both beam models.

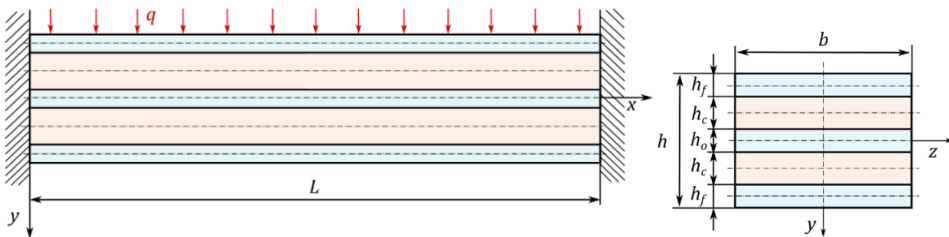


Fig. 1. Scheme of the five-layered composite beam and its cross-section

The variation of Young’s modulus in the depth direction of the five-layered composite beam is shown in Fig. 2.

Thus, Young’s modulus in the upper face ($-1/2 \leq \eta \leq -1/2 + \chi_f$), middle layer ($-\chi_0/2 \leq \eta \leq \chi_0/2$) and lower face ($1/2 - \chi_f \leq \eta \leq 1/2$) is constant – E_f , and similarly in the upper core ($-1/2 + \chi_f \leq \eta \leq -\chi_0/2$) and lower core ($\chi_0/2 \leq \eta \leq 1/2 - \chi_f$) is constant as well but has a different value – E_c , where:

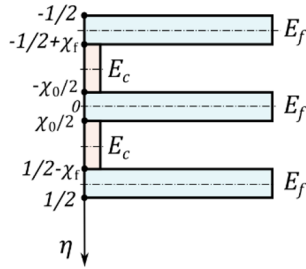


Fig. 2. Scheme of the variation of Young's modulus in the depth direction of the beam

$\eta = y/h$ – dimensionless coordinate, $\chi_f = h_f/h$, $\chi_c = h_c/h$, $\chi_0 = h_0/h$ – relative thicknesses of the beam layers.

2. The first model of the five-layered composite beam

The deformation of a planar cross-section of the composite beam in accordance with the zig-zag theory without the shear effect in the middle layer is shown in Fig. 3.

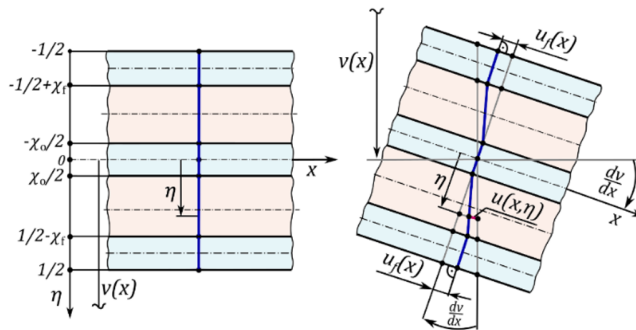


Fig. 3. The scheme of a planar cross-section deformation – the zig-zag theory

The longitudinal displacements following Fig. 3 in successive layers are as follows:

- the upper face ($-1/2 \leq \eta \leq -1/2 + \chi_f$)

$$u^{(uf)}(x, \eta) = -h \left[\eta \frac{dv}{dx} + \psi_f(x) \right], \quad (1)$$

- the upper core ($-1/2 + \chi_f \leq \eta \leq -\chi_0/2$)

$$u^{(uc)}(x, \eta) = -h \left[\eta \frac{dv}{dx} - \left(\eta + \frac{1}{2} \chi_0 \right) \frac{\psi_f(x)}{\chi_c} \right], \quad (2)$$

- the middle layer ($-\chi_0/2 \leq \eta \leq \chi_0/2$)

$$u^{(ml)}(x, \eta) = -h\eta \frac{dv}{dx}, \quad (3)$$

- the lower core ($\chi_0/2 \leq \eta \leq 1/2 - \chi_f$)

$$u^{(lc)}(x, \eta) = -h \left[\eta \frac{dv}{dx} - \left(\eta - \frac{1}{2}\chi_0 \right) \frac{\psi_f(x)}{\chi_c} \right], \quad (4)$$

- the lower face ($1/2 - \chi_f \leq \eta \leq 1/2$)

$$u^{(lf)}(x, \eta) = -h \left[\eta \frac{dv}{dx} - \psi_f(x) \right], \quad (5)$$

where: $v(x)$ – deflection, $\psi_f(x) = u_f(x)/h$ – dimensionless function of the shear effect.

Therefore, the strains and stresses – Hooke's law are as follows:

- the upper face ($-1/2 \leq \eta \leq -1/2 + \chi_f$)

$$\varepsilon_x^{(uf)}(x, \eta) = -h \left[\eta \frac{d^2v}{dx^2} + \frac{d\psi_f}{dx} \right], \quad (6a)$$

$$\gamma_{xy}^{(uf)}(x, \eta) = 0, \quad (6b)$$

$$\sigma_x^{(uf)}(x, \eta) = E_f \varepsilon_x^{(uf)}(x, \eta), \quad (7a)$$

$$\tau_{xy}^{(uf)}(x, \eta) = 0, \quad (7b)$$

- the upper core ($-1/2 + \chi_f \leq \eta \leq -\chi_0/2$)

$$\varepsilon_x^{(uc)}(x, \eta) = -h \left[\eta \frac{d^2v}{dx^2} - \left(\eta + \frac{1}{2}\chi_0 \right) \frac{1}{\chi_c} \frac{d\psi_f}{dx} \right], \quad (8a)$$

$$\gamma_{xy}^{(uc)}(x, \eta) = \frac{\psi_f(x)}{\chi_c}, \quad (8b)$$

$$\sigma_x^{(uc)}(x, \eta) = E_c \varepsilon_x^{(uc)}(x, \eta), \quad (9a)$$

$$\tau_{xy}^{(uc)}(x, \eta) = \frac{E_c}{2(1 + \nu_c)} \gamma_{xy}^{(uc)}(x, \eta), \quad (9b)$$

- the middle layer ($-\chi_0/2 \leq \eta \leq \chi_0/2$)

$$\varepsilon_x^{(ml)}(x, \eta) = -h\eta \frac{d^2v}{dx^2}, \quad (10a)$$

$$\gamma_{xy}^{(ml)}(x, \eta) = 0, \quad (10b)$$

$$\sigma_x^{(ml)}(x, \eta) = E_f \varepsilon_x^{(ml)}(x, \eta), \quad (11a)$$

$$\tau_{xy}^{(ml)}(x, \eta) = 0, \quad (11b)$$

- the lower core ($\chi_0/2 \leq \eta \leq 1/2 - \chi_f$)

$$\varepsilon_x^{(lc)}(x, \eta) = -h \left[\eta \frac{d^2 v}{dx^2} - \left(\eta - \frac{1}{2} \chi_0 \right) \frac{1}{\chi_c} \frac{d\psi_f}{dx} \right], \quad (12a)$$

$$\gamma_{xy}^{(lc)}(x, \eta) = \frac{\psi_f(x)}{\chi_c}, \quad (12b)$$

$$\sigma_x^{(lc)}(x, \eta) = E_c \varepsilon_x^{(lc)}(x, \eta), \quad (13a)$$

$$\tau_{xy}^{(lc)}(x, \eta) = \frac{E_c}{2(1 + \nu_c)} \gamma_{xy}^{(lc)}(x, \eta), \quad (13b)$$

- the lower face ($1/2 - \chi_f \leq \eta \leq 1/2$)

$$\varepsilon_x^{(lf)}(x, \eta) = -h \left[\eta \frac{d^2 v}{dx^2} - \frac{d\psi_f}{dx} \right], \quad (14a)$$

$$\gamma_{xy}^{(lf)}(x, \eta) = 0, \quad (14b)$$

$$\sigma_x^{(lf)}(x, \eta) = E_f \varepsilon_x^{(lf)}(x, \eta), \quad (15a)$$

$$\tau_{xy}^{(lf)}(x, \eta) = 0, \quad (15b)$$

where ν_c – Poisson's ratio of the cores.

The elastic strain energy is in the form

$$\begin{aligned}
 U_{\varepsilon, \gamma} = \frac{1}{2} E_f b h \int_0^L & \left[\Phi_{\varepsilon, \gamma}^{(uf)}(x) + \Phi_{\varepsilon, \gamma}^{(uc)}(x) + \Phi_{\varepsilon, \gamma}^{(ml)}(x) \right. \\
 & \left. + \Phi_{\varepsilon, \gamma}^{(lc)}(x) + \Phi_{\varepsilon, \gamma}^{(lf)}(x) \right] dx, \quad (16)
 \end{aligned}$$

where:

$$\Phi_{\varepsilon, \gamma}^{(uf)}(x) = \int_{-1/2}^{-1/2 + \chi_f} \left[\varepsilon_x^{(uf)}(x, \eta) \right]^2 d\eta, \quad \Phi_{\varepsilon, \gamma}^{(lf)}(x) = \int_{1/2 - \chi_f}^{1/2} \left[\varepsilon_x^{(lf)}(x, \eta) \right]^2 d\eta,$$

$$\Phi_{\varepsilon, \gamma}^{(uc)}(x) = e_c \int_{-1/2 + \chi_f}^{-\chi_0/2} \left\{ \left[\varepsilon_x^{(uc)}(x, \eta) \right]^2 + \frac{1}{2(1 + \nu_c)} \left[\gamma_{xy}^{(uc)}(x, \eta) \right]^2 \right\} d\eta,$$

$$\Phi_{\varepsilon, \gamma}^{(lc)}(x) = e_c \int_{\chi_0/2}^{1/2 - \chi_f} \left\{ \left[\varepsilon_x^{(lc)}(x, \eta) \right]^2 + \frac{1}{2(1 + \nu_c)} \left[\gamma_{xy}^{(lc)}(x, \eta) \right]^2 \right\} d\eta,$$

$$\Phi_{\varepsilon,\gamma}^{(ml)}(x) = \int_{-\chi_0/2}^{\chi_0/2} \left[\varepsilon_x^{(ml)}(x, \eta) \right]^2 d\eta.$$

Substituting the expressions (6a), (6b), (8a), (8b), (10a), (10b), (12a), (12b), (14a), (14b) for strains into the expressions (16), after integration one obtains

$$U_{\varepsilon,\gamma} = \frac{E_f b h^3}{24} \int_0^L \left[C_{vv} \left(\frac{d^2 v}{dx^2} \right)^2 - 2C_{v\psi} \frac{d^2 v}{dx^2} \frac{d\psi_f}{dx} + C_{\psi\psi} \left(\frac{d\psi_f}{dx} \right)^2 + C_{\psi} \frac{\psi_f^2(x)}{h^2} \right] dx, \quad (17)$$

where dimensionless coefficients are expressed as:

$$C_{vv} = 2 \left(3 - 6\chi_f + 4\chi_f^2 \right) \chi_f + e_c (1 - 2\chi_f)^3 + (1 - e_c) \chi_0^3,$$

$$C_{v\psi} = \frac{1}{2} \left\{ 24 (1 - \chi_f) \chi_f + e_c \left[2 (1 - 2\chi_f)^3 - 3 (1 - 2\chi_f)^2 \chi_0 + \chi_0^3 \right] \frac{1}{\chi_c} \right\},$$

$$C_{\psi\psi} = 8 (3\chi_f + e_c \chi_c), \quad C_{\psi} = \frac{12}{1 + \nu_c} \frac{e_c}{\chi_c}.$$

The work of the load

$$W = \int_0^L q v(x) dx. \quad (18)$$

Based on the principle of stationary total potential energy $\delta(U_{\varepsilon,\gamma} - W) = 0$, the system of two differential equations of equilibrium of this beam is obtained in the following form:

$$C_{vv} \frac{d^4 v}{dx^4} - C_{v\psi} \frac{d^3 \psi_f}{dx^3} = 12 \frac{q}{E_f b h^3}, \quad (19)$$

$$C_{v\psi} \frac{d^3 v}{dx^3} - C_{\psi\psi} \frac{d^2 \psi_f}{dx^2} + C_{\psi} \frac{\psi_f(x)}{h^2} = 0. \quad (20)$$

It may be easily noticed, that the equation (19) of this system is equivalent to the second-order equation of the form

$$C_{vv} \frac{d^2 v}{dx^2} - C_{v\psi} \frac{d\psi_f}{dx} = -12 \frac{M_b(x)}{E_f b h^3}, \quad (21)$$

where $M_b(x) = -M_o + 1/2 (Lx - x^2) q$ – the bending moment (Fig. 4). Differentiating the above equation (21) twice, with consideration of this expression for

the bending moment, where $d^2 M_b/dx^2 = -q$, the equation (19) is obtained. This problem of the equivalence of such two equations is presented, for example, in paper [22].

Therefore, equations (21) and (20) are the governing equations of this beam bending. These two equations are reduced to one equation in the form

$$\frac{d^2 \psi_f}{d\xi^2} - (\alpha\lambda)^2 \psi_f(\xi) = -\frac{C_{v\psi}}{C_{vv}C_{\psi\psi} - C_{v\psi}^2} \lambda^2 \frac{T(\xi)}{E_f b h}, \quad (22)$$

where: $\xi = x/L$ – dimensionless coordinate, $\lambda = L/h$ – relative length of the beam,

$\alpha = \sqrt{\frac{C_{vv}C_{\psi\psi}}{C_{vv}C_{\psi\psi} - C_{v\psi}^2}}$ – dimensionless coefficient and $T(\xi)$ – shear force.

The scheme of the end part of the beam with the load and reactions is shown in Fig. 4.

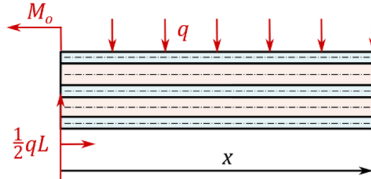


Fig. 4. Scheme of the end part of the beam with the load and reactions

Taking into account the above scheme, the shear force and the bending moment in dimensionless coordinate ξ are as follows:

$$T(\xi) = \frac{1}{2} (1 - 2\xi) qL, \quad (23a)$$

$$M_b(\xi) = \frac{1}{2} (\xi - \xi^2 - 2\bar{M}_o) qL^2, \quad (23b)$$

where the dimensionless reaction moment $\bar{M}_o = M_o/qL^2$.

The solution of equation (22), with consideration of the expression (23a) for the shear force and conditions $\psi_f(0) = 0$, $\psi_f(1/2) = 0$, is the following dimensionless function

$$\psi_f(\xi) = \bar{\psi}_f(\xi) \frac{q}{E_f b}, \quad (24)$$

where the relative dimensionless function of the shear effect

$$\bar{\psi}_f(\xi) = 6 \left\{ 1 - 2\xi - \frac{\sinh[(1 - 2\xi)\alpha\lambda/2]}{\sinh(\alpha\lambda/2)} \right\} \frac{C_{v\psi}}{C_{vv}C_{\psi}} \lambda. \quad (25)$$

The equation (21) in dimensionless coordinate ξ , with consideration of the expression (23b) for the bending moment, is as follows

$$C_{vv} \frac{d^2 \bar{\psi}}{d\xi^2} = C_{v\psi} \frac{d\psi_f}{d\xi} - 6 (\xi - \xi^2 - 2\bar{M}_o) \lambda^3 \frac{q}{E_f b}, \quad (26)$$

where $\bar{v}(\xi) = v(\xi)/L$ – relative deflection.

Integrating this equation twice, taking into account the function (24) and the following conditions $d\bar{v}/d\xi|_0 = 0$, $d\bar{v}/d\xi|_{1/2} = 0$, $\bar{v}(0) = 0$, the beam deflection line was obtained of the form

$$\bar{v}(\xi) = \tilde{v}(\xi) \frac{q}{E_f b}, \quad (27)$$

where:

$$\tilde{v}(\xi) = \left[f_\psi(\xi) - \frac{1}{2} (2\xi - \xi^2 - 1) \xi^2 \right] \frac{\lambda^3}{C_{vv}}, \quad (28a)$$

$$f_\psi(\xi) = 6 \left\{ \xi - \xi^2 - \frac{\cosh(\alpha\lambda/2) - \cosh[(1-2\xi)\alpha\lambda/2]}{\alpha\lambda \sinh(\alpha\lambda/2)} \right\} \frac{C_{v\psi}^2}{C_{vv} C_\psi} \frac{1}{\lambda^2}, \quad (28b)$$

and the dimensionless reaction moment $\bar{M}_o = 1/12$.

Thus, the relative maximum deflection

$$\bar{v}_{\max} = \bar{v} \left(\frac{1}{2} \right) = \tilde{v}_{\max} \frac{q}{E_f b}, \quad (29)$$

where dimensionless relative maximum deflection

$$\tilde{v}_{\max} = \tilde{v} \left(\frac{1}{2} \right) = (1 + C_{se}) \frac{\lambda^3}{32 C_{vv}}, \quad (30)$$

and the shear coefficient

$$C_{se} = 48 \left[1 - 4 \frac{\cosh(\alpha\lambda/2)}{\alpha\lambda \sinh(\alpha\lambda/2)} \right] \frac{C_{v\psi}^2}{C_{vv} C_\psi} \frac{1}{\lambda^2}, \quad (31)$$

Exemplary calculations are carried out for three beam structures (S-1, S-2, S-3) of the same mass for selected following dimensionless sizes: $\lambda = 30$, $\chi_f = (3/24, 2.5/24, 2/24)$, $\chi_c = 9/24$, $\chi_0 = (0, 1/24, 2/24)$ and material constant $\nu_c = 0.3$, $e_c = 1/40$. The results of the calculations of the values of shear coefficient C_{se} (31), and maximum deflection \tilde{v}_{\max} (30) are specified in Table 1.

Table 1. The values of shear coefficient C_{se} and maximum deflection \tilde{v}_{\max} – first model

Structure	S-1	S-2	S-3
χ_f	3/24	2.5/24	2/24
χ_0	0	1/24	2/24
C_{se}	0.2579	0.2179	0.1762
\tilde{v}_{\max}	1803.0	1990.3	2274.5

The shear stresses (7), (11) and (15) in the upper face, middle layer, and lower face are equal to zero. Whereas, the shear stresses (9) and (13) in the

upper core ($-1/2 + \chi_f \leq \eta \leq -\chi_0/2$) and lower core ($\chi_0/2 \leq \eta \leq 1/2 - \chi_f$) with consideration of the function (24) are the same as follows

$$\tau_{xy}^{(uc)}(\xi, \eta) = \tau_{xy}^{(lc)}(\xi, \eta) = \bar{\tau}_{xy}^{(c)}(\xi, \eta) \frac{q}{b}, \quad (32)$$

where, the dimensionless shear stress

$$\bar{\tau}_{xy}^{(c)}(\xi, \eta) = \frac{1}{2(1 + \nu)} \frac{e_c}{\chi_c} \bar{\psi}_f(\xi). \quad (33)$$

Exemplary calculations are carried out for the beam of selected following dimensionless sizes: $\lambda = 30$, $\chi_f = 2/24$, $\chi_c = 9/24$, $\chi_0 = 2/24$ and material constant $\nu_c = 0.3$, $e_c = 1/40$. The results of the calculations – the graphs of the relative dimensionless function of the shear effect (25) $\bar{\psi}_f(\xi)$ and the dimensionless shear stress (33) $\bar{\tau}_{xy}^{(c)}(0.05, \eta)$ for $\xi = 0.05$ [$\bar{\psi}_f(0.05) = 572.847$], are shown in Fig. 5 and Fig. 6.

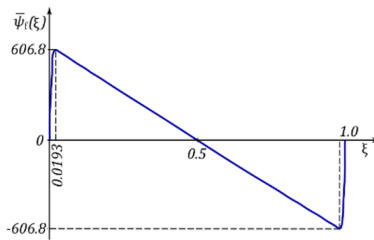


Fig. 5. Scheme of the end part of the beam with the load and reactions $\bar{\psi}_f(\xi)$

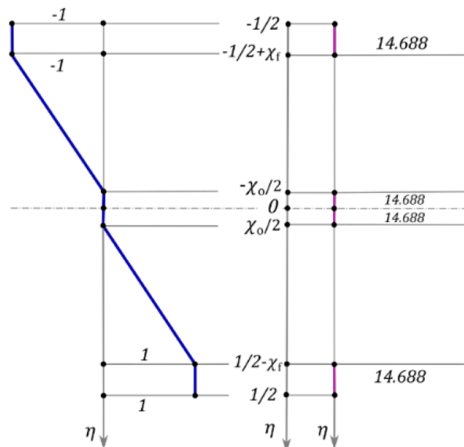


Fig. 6. The graphs of the planar cross-section deformation and the dimensionless shear stress $\bar{\tau}_{xy}^{(c)}(0.05, \eta)$ for $\xi = 0.05$

3. The second model of the five-layered composite beam

The deformation of a planar cross-section of the composite beam in accordance with the nonlinear shear deformation theory is shown in Fig. 7.

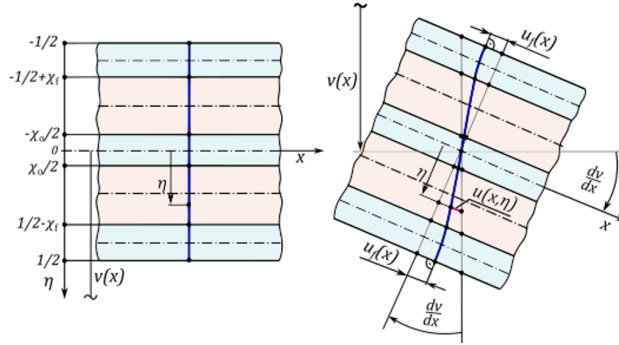


Fig. 7. The scheme of a planar cross-section deformation – nonlinear shear deformation theory

The longitudinal displacements according to Fig. 7 and also the strains and stresses in successive layers are as follows:

- the upper face ($-1/2 \leq \eta \leq -1/2 + \chi_f$)

$$u^{(uf)}(x, \eta) = -h \left[\eta \frac{dv}{dx} - f_d^{(uf)}(\eta) \psi_f(x) \right]. \quad (34)$$

$$\varepsilon_x^{(uf)}(x, \eta) = -h \left[\eta \frac{d^2v}{dx^2} - f_d^{(uf)}(\eta) \frac{d\psi_f}{dx} \right], \quad (35a)$$

$$\gamma_{xy}^{(uf)}(x, \eta) = \frac{df_d^{(uf)}}{d\eta} \psi_f(x), \quad (35b)$$

$$\sigma_x^{(uf)}(x, \eta) = E_f \varepsilon_x^{(uf)}(x, \eta), \quad (36a)$$

$$\tau_{xy}^{(uf)}(x, \eta) = \frac{E_f}{2(1 + \nu_f)} \gamma_{xy}^{(uf)}(x, \eta), \quad (36b)$$

- the upper core ($-1/2 + \chi_f \leq \eta \leq -\chi_0/2$)

$$u^{(uc)}(x, \eta) = -h \left[\eta \frac{dv}{dx} - f_d^{(uc)}(\eta) \psi_f(x) \right], \quad (37)$$

$$\varepsilon_x^{(uc)}(x, \eta) = -h \left[\eta \frac{d^2v}{dx^2} - f_d^{(uc)}(\eta) \frac{d\psi_f}{dx} \right], \quad (38a)$$

$$\gamma_{xy}^{(uc)}(x, \eta) = \frac{df_d^{(uc)}}{d\eta} \psi_f(x), \quad (38b)$$

$$\sigma_x^{(uc)}(x, \eta) = E_c \varepsilon_x^{(uf)}(x, \eta), \quad (39a)$$

$$\tau_{xy}^{(uc)}(x, \eta) = \frac{E_c}{2(1 + \nu_c)} \gamma_{xy}^{(uc)}(x, \eta), \quad (39b)$$

- the middle layer ($-\chi_0/2 \leq \eta \leq \chi_0/2$)

$$u^{(ml)}(x, \eta) = -h \left[\eta \frac{dv}{dx} - f_d^{(ml)}(\eta) \psi_f(x) \right], \quad (40)$$

$$\varepsilon_x^{(ml)}(x, \eta) = -h \left[\eta \frac{d^2v}{dx^2} - f_d^{(ml)}(\eta) \frac{d\psi_f}{dx} \right], \quad (41a)$$

$$\gamma_{xy}^{(ml)}(x, \eta) = \frac{df_d^{(ml)}}{d\eta} \psi_f(x), \quad (41b)$$

$$\sigma_x^{(ml)}(x, \eta) = E_f \varepsilon_x^{(ml)}(x, \eta), \quad (42a)$$

$$\tau_{xy}^{(ml)}(x, \eta) = \frac{E_f}{2(1 + \nu_f)} \gamma_{xy}^{(ml)}(x, \eta), \quad (42b)$$

- the lower core ($\chi_0/2 \leq \eta \leq 1/2 - \chi_f$)

$$u^{(lc)}(x, \eta) = -h \left[\eta \frac{dv}{dx} - f_d^{(lc)}(\eta) \psi_f(x) \right], \quad (43)$$

$$\varepsilon_x^{(lc)}(x, \eta) = -h \left[\eta \frac{d^2v}{dx^2} - f_d^{(lc)}(\eta) \frac{d\psi_f}{dx} \right], \quad (44a)$$

$$\gamma_{xy}^{(lc)}(x, \eta) = \frac{df_d^{(lc)}}{d\eta} \psi_f(x), \quad (44b)$$

$$\sigma_x^{(lc)}(x, \eta) = E_f \varepsilon_x^{(lc)}(x, \eta), \quad (45a)$$

$$\tau_{xy}^{(lc)}(x, \eta) = \frac{E_c}{2(1 + \nu_c)} \gamma_{xy}^{(lc)}(x, \eta), \quad (45b)$$

- the lower face ($1/2 - \chi_f \leq \eta \leq 1/2$)

$$u^{(lf)}(x, \eta) = -h \left[\eta \frac{dv}{dx} - f_d^{(lf)}(\eta) \psi_f(x) \right], \quad (46)$$

$$\varepsilon_x^{(lf)}(x, \eta) = -h \left[\eta \frac{d^2v}{dx^2} - f_d^{(lf)}(\eta) \frac{d\psi_f}{dx} \right], \quad (47a)$$

$$\gamma_{xy}^{(lf)}(x, \eta) = \frac{d f_d^{(lf)}}{d \eta} \psi_f(x), \quad (47b)$$

$$\sigma_x^{(lf)}(x, \eta) = E_f \varepsilon_x^{(lf)}(x, \eta), \quad (48a)$$

$$\tau_{xy}^{(lf)}(x, \eta) = \frac{E_f}{2(1 + \nu_f)} \gamma_{xy}^{(lf)}(x, \eta), \quad (48b)$$

where: $f_d^{(uf)}(\eta)$, $f_d^{(uc)}(\eta)$, $f_d^{(ml)}(\eta)$, $f_d^{(lc)}(\eta)$, $f_d^{(lf)}(\eta)$ – unknown dimensionless deformation functions, and ν_f – Poisson's ratio of the faces.

Taking into account the papers [21, 22] these functions are determined considering the classical shear stress formula in the following form

$$\tau_{xy}^{(Cl)}(x, y) = \frac{S_z(y) T(x)}{b(y) J_z}, \quad (49)$$

where: $S_z(y)$ – the first moment of the cross-section area part, $b(y)$ – width of the cross-section, $T(x)$ – shear force, J_z – inertia moment of the beam cross-section.

This formula, for a rectangular cross-section $b(y) = b$ and in the dimensionless coordinate $\eta = y/h$, is as follows

$$\tau_{xy}^{(Cl)}(x, \eta) = \bar{S}_z(\eta) \frac{T(x)}{J_z} h^2, \quad (50)$$

where $\bar{S}_z(\eta)$ – dimensionless first moment considering the variation of Young's modulus in the depth direction of the five-layered composite beam.

Therefore, this moment for the upper face ($-1/2 \leq \eta \leq -1/2 + \chi_f$) is formulated based on the following scheme (Fig. 8).

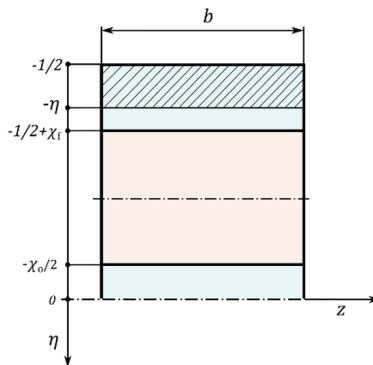


Fig. 8. The hatched area of the selected part of the upper face

Thus, the dimensionless first moment of the hatched area is in the form

$$\bar{S}_z^{(uf)}(\eta) = \frac{1}{2} \left(\frac{1}{4} - \eta^2 \right). \quad (51)$$

Proceeding analogously for successive layers, the first moment is as follows:

- the upper core ($-1/2 + \chi_f \leq \eta \leq -\chi_0/2$)

$$\bar{S}_z^{(uc)}(\eta) = \frac{1}{2} \left\{ (1 - \chi_f) \chi_f + e_c \left[\left(\frac{1}{2} - \chi_f \right)^2 - \eta^2 \right] \right\}, \quad (52)$$

- the middle layer ($-\chi_0/2 \leq \eta \leq \chi_0/2$)

$$\bar{S}_z^{(ml)}(\eta) = \frac{1}{2} \left\{ (1 - \chi_f) \chi_f + e_c \left[\left(\frac{1}{2} - \chi_f \right)^2 - \frac{1}{4} \chi_0^2 \right] + \frac{1}{4} \chi_0^2 - \eta^2 \right\}, \quad (53)$$

- the lower core ($\chi_0/2 \leq \eta \leq 1/2 - \chi_f$)

$$\bar{S}_z^{(lc)}(\eta) = \frac{1}{2} \left\{ (1 - \chi_f) \chi_f + e_c \left[\left(\frac{1}{2} - \chi_f \right)^2 - \eta^2 \right] \right\}, \quad (54)$$

- the lower face ($1/2 - \chi_f \leq \eta \leq 1/2$)

$$\bar{S}_z^{(lf)}(\eta) = \frac{1}{2} \left(\frac{1}{4} - \eta^2 \right). \quad (55)$$

Equating the shear stresses (36b), (39b), (42b), (45b), and (48b) to the classical shear stress formula (50) with consideration of the dimensionless first moments (51), (52), (53), (54) and (55) one obtains the unknown dimensionless deformation functions in the following form:

- the upper face ($-1/2 \leq \eta \leq -1/2 + \chi_f$)

$$f_d^{(uf)}(\eta) = C_{uf} + (1 + \nu_f) \left(\frac{1}{4} - \frac{1}{3} \eta^2 \right) \eta, \quad (56)$$

- the upper core ($-1/2 + \chi_f \leq \eta \leq -\chi_0/2$)

$$f_d^{(uc)}(\eta) = C_{uc} + \frac{1 + \nu_c}{e_c} \left\{ (1 - \chi_f) \chi_f + e_c \left[(1 - \chi_f)^2 - \frac{1}{3} \eta^2 \right] \right\} \eta, \quad (57)$$

- the middle layer ($-\chi_0/2 \leq \eta \leq \chi_0/2$)

$$f_d^{(ml)}(\eta) = (1 + \nu_f) \left\{ (1 - \chi_f) \chi_f + e_c \left[\left(\frac{1}{2} - \chi_f \right)^2 - \frac{1}{4} \chi_0^2 \right] + \frac{1}{4} \chi_0^2 - \frac{1}{3} \eta^2 \right\} \eta, \quad (58)$$

- the lower core ($\chi_0/2 \leq \eta \leq 1/2 - \chi_f$)

$$f_d^{(lc)}(\eta) = C_{lc} + \frac{1 + \nu_c}{e_c} \left\{ (1 - \chi_f) \chi_f + e_c \left[(1 - \chi_f)^2 - \frac{1}{3} \eta^2 \right] \right\} \eta, \quad (59)$$

- the lower face ($1/2 - \chi_f \leq \eta \leq 1/2$)

$$f_d^{(lf)}(\eta) = C_{lf} + (1 + \nu_f) \left(\frac{1}{4} - \frac{1}{3}\eta^2 \right) \eta, \quad (60)$$

where:

$$C_{uc} = -C_{lc} = \frac{1}{2} \left[\frac{1 + \nu_c}{e_c} C_{c1} - (1 + \nu_f) C_{c2} \right] \chi_0,$$

$$C_{c1} = (1 - \chi_f) \chi_f + e_c \left[\left(\frac{1}{2} - \chi_f \right)^2 - \frac{1}{12} \chi_0^2 \right],$$

$$C_{c2} = (1 - \chi_f) \chi_f + e_c \left[\left(\frac{1}{2} - \chi_f \right)^2 - \frac{1}{4} \chi_0^2 \right] + \frac{1}{6} \chi_0^2,$$

$$C_{c3} = 3 (1 - \chi_f) \chi_f + 2e_c \left(\frac{1}{2} - \chi_f \right)^2,$$

$$C_{uf} = -C_{lf} = C_{uc} - \frac{1}{6} \left\{ 2 \frac{1 + \nu_c}{e_c} C_{c3} - (1 + \nu_f) [1 + 2 (1 - \chi_f) \chi_f] \right\} \left(\frac{1}{2} - \chi_f \right).$$

Importantly, the derived functions satisfy the continuity conditions between successive layers.

The elastic strain energy is in the form

$$U_{\varepsilon, \gamma} = \frac{1}{2} E_f b h \int_0^L \left[\Theta_{\varepsilon, \gamma}^{(uf)}(x) + \Theta_{\varepsilon, \gamma}^{(uc)}(x) + \Theta_{\varepsilon, \gamma}^{(ml)}(x) + \Theta_{\varepsilon, \gamma}^{(lc)}(x) + \Theta_{\varepsilon, \gamma}^{(lf)}(x) \right] dx, \quad (61)$$

where:

$$\Theta_{\varepsilon, \gamma}^{(uf)}(x) = \int_{-1/2}^{-1/2 + \chi_f} \left\{ \left[\varepsilon_x^{(uf)}(x, \eta) \right]^2 + \frac{1}{2(1 + \nu_f)} \left[\gamma_{xy}^{(uf)}(x, \eta) \right]^2 \right\} d\eta,$$

$$\Theta_{\varepsilon, \gamma}^{(uc)}(x) = e_c \int_{-1/2 + \chi_f}^{-\chi_0/2} \left\{ \left[\varepsilon_x^{(uc)}(x, \eta) \right]^2 + \frac{1}{2(1 + \nu_c)} \left[\gamma_{xy}^{(uc)}(x, \eta) \right]^2 \right\} d\eta,$$

$$\Theta_{\varepsilon, \gamma}^{(ml)}(x) = \int_{-\chi_0/2}^{\chi_0/2} \left\{ \left[\varepsilon_x^{(ml)}(x, \eta) \right]^2 + \frac{1}{2(1 + \nu_f)} \left[\gamma_{xy}^{(ml)}(x, \eta) \right]^2 \right\} d\eta,$$

$$\Theta_{\varepsilon, \gamma}^{(lc)}(x) = e_c \int_{\chi_0/2}^{1/2 - \chi_f} \left\{ \left[\varepsilon_x^{(lc)}(x, \eta) \right]^2 + \frac{1}{2(1 + \nu_c)} \left[\gamma_{xy}^{(lc)}(x, \eta) \right]^2 \right\} d\eta,$$

$$\Theta_{\varepsilon, \gamma}^{(lf)}(x) = \int_{1/2-\chi_f}^{1/2} \left\{ \left[\varepsilon_x^{(lf)}(x, \eta) \right]^2 + \frac{1}{2(1+\nu_f)} \left[\gamma_{xy}^{(lf)}(x, \eta) \right]^2 \right\} d\eta.$$

Substituting the expressions (35), (38), (41), (44), (47) for strains into the expressions (61), after integration one obtains

$$U_{\varepsilon, \gamma} = \frac{E_f b h^3}{24} \int_0^L \left[C_{vv} \left(\frac{d^2 v}{dx^2} \right)^2 - 2C_{v\psi} \frac{d^2 v}{dx^2} \frac{d\psi_f}{dx} + C_{\psi\psi} \left(\frac{d\psi_f}{dx} \right)^2 + C_{\psi} \frac{\psi_f^2(x)}{h^2} \right] dx, \quad (62)$$

where dimensionless coefficients

$$\begin{aligned} C_{vv} &= 2 \left(3 - 6\chi_f + 4\chi_f^2 \right) \chi_f + e_c (1 - 2\chi_f)^3 + (1 - e_c) \chi_0^3, \\ C_{v\psi} &= 12 \left[J_{v\psi}^{(uf)} + e_c J_{v\psi}^{(uc)} + J_{v\psi}^{(ml)} + e_c J_{v\psi}^{(lc)} + J_{v\psi}^{(lf)} \right], \\ C_{\psi\psi} &= 12 \left[J_{\psi\psi}^{(uf)} + e_c J_{\psi\psi}^{(uc)} + J_{\psi\psi}^{(ml)} + e_c J_{\psi\psi}^{(lc)} + J_{\psi\psi}^{(lf)} \right], \\ C_{\psi} &= 24 \left[(1+\nu_f) J_{\psi}^{(uf)} + \frac{1+\nu_c}{e_c} J_{\psi}^{(uc)} + (1+\nu_f) J_{\psi}^{(ml)} + \frac{1+\nu_c}{e_c} J_{\psi}^{(lc)} + (1+\nu_f) J_{\psi}^{(lf)} \right], \\ J_{v\psi}^{(uf)} &= \int_{-1/2}^{-1/2+\chi_f} \eta f_d^{(uf)}(\eta) d\eta, \quad J_{v\psi}^{(uc)} = \int_{-1/2+\chi_f}^{-\chi_0/2} \eta f_d^{(uc)}(\eta) d\eta, \quad J_{v\psi}^{(ml)} = \int_{-\chi_0/2}^{\chi_0/2} \eta f_d^{(ml)}(\eta) d\eta, \\ J_{v\psi}^{(lc)} &= \int_{\chi_0/2}^{1/2-\chi_f} \eta f_d^{(lc)}(\eta) d\eta, \quad J_{v\psi}^{(lf)} = \int_{1/2-\chi_f}^{1/2} \eta f_d^{(lf)}(\eta) d\eta, \quad J_{\psi\psi}^{(uf)} = \int_{-1/2}^{-1/2+\chi_f} \left[f_d^{(uf)}(\eta) \right]^2 d\eta, \\ J_{\psi\psi}^{(uc)} &= \int_{-1/2+\chi_f}^{-\chi_0/2} \left[f_d^{(uc)}(\eta) \right]^2 d\eta, \quad J_{\psi\psi}^{(ml)} = \int_{-\chi_0/2}^{\chi_0/2} \left[f_d^{(ml)}(\eta) \right]^2 d\eta, \quad J_{\psi\psi}^{(lc)} = \int_{\chi_0/2}^{1/2-\chi_f} \left[f_d^{(lc)}(\eta) \right]^2 d\eta, \\ J_{\psi\psi}^{(lf)} &= \int_{1/2-\chi_f}^{1/2} \left[f_d^{(lf)}(\eta) \right]^2 d\eta, \quad J_{\psi}^{(uf)} = \int_{-1/2}^{-1/2+\chi_f} \left[\bar{S}_z^{(uf)}(\eta) \right]^2 d\eta, \quad J_{\psi}^{(uc)} = \int_{-1/2+\chi_f}^{-\chi_0/2} \left[\bar{S}_z^{(uc)}(\eta) \right]^2 d\eta, \end{aligned}$$

$$J_{\psi}^{(ml)} = \int_{-\chi_0/2}^{\chi_0/2} [\bar{S}_z^{(ml)}(\eta)]^2 d\eta, \quad J_{\psi}^{(lc)} = \int_{\chi_0/2}^{1/2-\chi_f} [\bar{S}_z^{(lc)}(\eta)]^2 d\eta, \quad J_{\psi}^{(lf)} = \int_{1/2-\chi_f}^{1/2} [\bar{S}_z^{(lf)}(\eta)]^2 d\eta.$$

Thus, based on the principle of stationary total potential energy $\delta(U_{\varepsilon,\gamma} - W) = 0$, with consideration of the expression (18) and after a simple transformation, the system of two differential equations governing the bending of this beam is obtained in the following form:

$$C_{vv} \frac{d^2 v}{dx^2} - C_{v\psi} \frac{d\psi_f}{dx} = -12 \frac{M_b(x)}{E_f b h^3}, \quad (63)$$

$$C_{v\psi} \frac{d^3 v}{dx^3} - C_{\psi\psi} \frac{d^2 \psi_f}{dx^2} + C_{\psi} \frac{\psi_f(x)}{h^2} = 0. \quad (64)$$

The form of these equations is identical to those in the first beam model. Therefore, taking into account the solution of this system in the first model was written:

a) the relative dimensionless function of the shear effect

$$\bar{\psi}_f(\xi) = 6 \left\{ 1 - 2\xi - \frac{\sinh[(1-2\xi)\alpha\lambda/2]}{\sinh(\alpha\lambda/2)} \right\} \frac{C_{v\psi}}{C_{vv}C_{\psi}} \lambda, \quad (65)$$

b) the shear coefficient

$$C_{se} = 48 \left[1 - 4 \frac{\cosh(\alpha\lambda/2)}{\alpha\lambda \sinh(\alpha\lambda/2)} \right] \frac{C_{v\psi}^2}{C_{vv}C_{\psi}} \frac{1}{\lambda^2}, \quad (66)$$

c) the dimensionless relative maximum deflection

$$\tilde{v}_{\max} = \tilde{v} \left(\frac{1}{2} \right) = (1 + C_{se}) \frac{\lambda^3}{32C_{vv}}. \quad (67)$$

Exemplary calculations are carried out for the same three beam structures as in the first model, i.e. dimensionless sizes: $\lambda = 30$, $\chi_f = (3/24, 2.5/24, 2/24)$, $\chi_c = 9/24$, $\chi_0 = (0, 1/24, 2/24)$ and material constant $\nu_c = 0.3$, $\nu_f = 0.33$, $e_c = 1/40$. The results of the calculations of the values of shear coefficient C_{se} (66), and maximum deflection \tilde{v}_{\max} (67) are specified in Table 2.

Moreover, the dimensionless shear stresses in successive layers are as follows

• the upper face $(-1/2 \leq \eta \leq -1/2 + \chi_f)$

$$\tau_{xy}^{(uf)}(x, \eta) = \bar{S}_z^{(uf)}(\eta) \psi_f(x), \quad (68)$$

Table 2. The values of shear coefficient C_{se} and maximum deflection \tilde{v}_{\max} – second model

Structure	S-1	S-2	S-3
χ_f	3/24	2.5/24	2/24
χ_0	0	1/24	2/24
C_{se}	0.2588	0.2191	0.1776
\tilde{v}_{\max}	1804.3	1992.3	2277.4

- the upper core ($-1/2 + \chi_f \leq \eta \leq -\chi_0/2$)

$$\tau_{xy}^{(uc)}(x, \eta) = \bar{S}_z^{(uc)}(\eta) \psi_f(x), \quad (69)$$

- the middle layer ($-\chi_0/2 \leq \eta \leq \chi_0/2$)

$$\tau_{xy}^{(ml)}(x, \eta) = \bar{S}_z^{(ml)}(\eta) \psi_f(x), \quad (70)$$

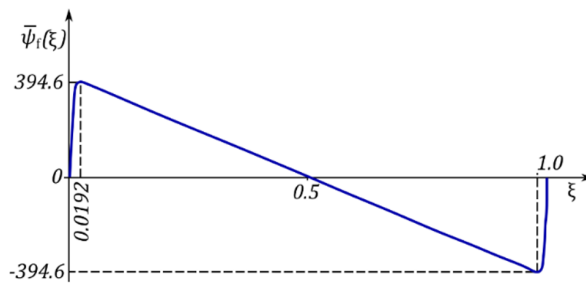
- the lower core ($\chi_0/2 \leq \eta \leq 1/2 - \chi_f$)

$$\tau_{xy}^{(lc)}(x, \eta) = \bar{S}_z^{(lc)}(\eta) \psi_f(x), \quad (71)$$

- the lower face ($1/2 - \chi_f \leq \eta \leq 1/2$)

$$\tau_{xy}^{(lf)}(x, \eta) = \bar{S}_z^{(lf)}(\eta) \psi_f(x). \quad (72)$$

Exemplary calculations are carried out for the beam of the selected following dimensionless sizes: $\lambda = 30$, $\chi_f = 2/24$, $\chi_c = 9/24$, $\chi_0 = 2/24$ and material constant $\nu_c = 0.3$, $e_c = 1/40$. The results of the calculations – the graphs of the relative dimensionless function of the shear effect (65) $\bar{\psi}_f(\xi)$ and the dimensionless shear stresses (68)–(72) for $\xi = 0.05$ [$\bar{\psi}_f(0.05) = 372.389$], are shown in Fig. 9 and Fig. 10.

Fig. 9. The graph of the relative dimensionless function of the shear effect $\bar{\psi}_f(\xi)$

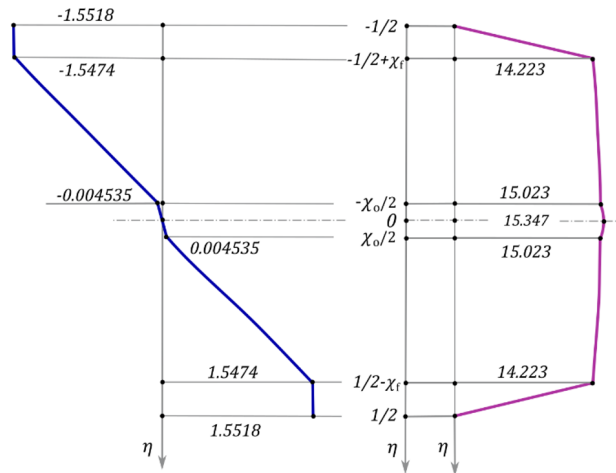


Fig. 10. The graphs of the planar cross-section deformation and the dimensionless shear stress $\bar{\tau}_{xy}^{(c)}(0.05, \eta)$ for $\xi = 0.05$

4. Conclusions

1. The values of the shear coefficient C_{se} and the dimensionless relative maximum deflection \tilde{v}_{\max} determined in both models (Table 1 and Table 2) differ slightly, these differences are less than 1%,
2. The shear stress distributions in the cross-section of the tested beam determined in both models differ significantly (Fig. 6, Fig. 10), while the difference between the maximum values of these stresses is small and amounts to 2.2%,
3. The second model of the beam refines the shear effect in the beam.

References

- [1] E. Carrera. Historical review of Zig-Zag theories for multilayered plates and shells. *Applied Mechanics Reviews*, 56(3):287–308, 2003. doi: [10.1115/1.1557614](https://doi.org/10.1115/1.1557614).
- [2] S.-J. Huang. An analytical method for calculating the stress and strain in adhesive layers in sandwich beams. *Composite Structures*, 60(1):105–114, 2003.
- [3] A. Pollien, Y. Condea, L. Pambaguian, and A. Mortensen. Graded open-cell aluminium foam core sandwich beams. *Materials Science and Engineering: A*, 404:9–18, 2005. doi: [10.1016/j.msea.2005.05.096](https://doi.org/10.1016/j.msea.2005.05.096).
- [4] H. Hu, S. Belouettar, M. Potier-Ferry, and E.M. Daya. Review and assessment of various theories for modeling sandwich composites. *Composite Structures*, 84(3):282–292, 2008. doi: [10.1016/j.compstruct.2007.08.007](https://doi.org/10.1016/j.compstruct.2007.08.007).
- [5] J.N. Reddy. Nonlocal nonlinear formulations for bending of classical and shear deformation theories of beams and plates. *International Journal of Engineering Science*, 48(11):1507–1518, 2010. doi: [10.1016/j.ijengsci.2010.09.020](https://doi.org/10.1016/j.ijengsci.2010.09.020).

- [6] A. Chakrabarti, H.D. Chalak, M.A. Iqbal, and A.H. Sheikh. A new FE model based on higher order zigzag theory for the analysis of laminated sandwich beam with soft core. *Composite Structures*, 93(2):271–279, 2011. doi: [10.1016/j.compstruct.2010.08.031](https://doi.org/10.1016/j.compstruct.2010.08.031).
- [7] E. Carrera, M. Filippi, and E. Zappino. Laminated beam analysis by polynomial, trigonometric, exponential and zig-zag theories. *European Journal of Mechanics A/Solids*, 41:58–69, 2013. doi: [10.1016/j.euromechsol.2013.02.006](https://doi.org/10.1016/j.euromechsol.2013.02.006).
- [8] K. Magnucki, M. Smyczyński, and P. Jasion. Deflection and strength of a sandwich beam with thin binding layers between faces and a core. *Archives of Mechanics*, 65(4):301–311, 2013.
- [9] M.J. Smyczyński, and E. Magnucka-Blandzi. Static and dynamic stability of an axially compressed five-layer sandwich beam. *Thin-Walled Structures*, 90:23–30, 2015. doi: [10.1016/j.tws.2015.01.005](https://doi.org/10.1016/j.tws.2015.01.005).
- [10] P. Paczos, P. Wasilewicz, and E. Magnucka-Blandzi. Experimental and numerical investigations of five-layered trapezoidal beams. *Composite Structures*, 145:129–141, 2016. doi: [10.1016/j.compstruct.2016.02.079](https://doi.org/10.1016/j.compstruct.2016.02.079).
- [11] U. Icardi, and F. Sola. Assessment of recent zig-zag theories for laminated and sandwich structures. *Composites Part B*, 97:26–52, 2016. doi: [10.1016/j.compositesb.2016.04.058](https://doi.org/10.1016/j.compositesb.2016.04.058).
- [12] E. Magnucka-Blandzi, Z. Walczak, P. Jasion, and L. Wittenbeck. Buckling and vibrations of metal sandwich beams with trapezoidal corrugated cores – the lengthwise corrugated main core. *Thin-Walled Structures*, 112:78–82, 2017. doi: [10.1016/j.tws.2016.12.013](https://doi.org/10.1016/j.tws.2016.12.013).
- [13] T.P. Vo, H.-T. Thai, T.-K. Nguyen, D. Lanc, and A. Karamanli. Flexural analysis of laminated composite and sandwich beams using a four-unknown shear and normal deformation theory. *Composite Structures*, 176:388–397, 2017. doi: [10.1016/j.compstruct.2017.05.041](https://doi.org/10.1016/j.compstruct.2017.05.041).
- [14] M.J. Smyczyński, and E. Magnucka-Blandzi. The three-point bending of a sandwich beam with two binding layers – Comparison of two nonlinear hypotheses. *Composite Structures*, 183:96–102, 2018. doi: [10.1016/j.compstruct.2017.01.065](https://doi.org/10.1016/j.compstruct.2017.01.065).
- [15] Y. Zhai, Y. Li, and S. Liang. Free vibration analysis of five-layered composite sandwich plates with two-layered viscoelastic cores. *Composite Structures*, 200:346–357, 2018. doi: [10.1016/j.compstruct.2018.05.082](https://doi.org/10.1016/j.compstruct.2018.05.082).
- [16] Y.L. Pei, P.S. Geng, and L.X. Li. A modified higher-order theory for FG beams. *European Journal of Mechanics A/Solids*, 72:186–197, 2018. doi: [10.1016/j.euromechsol.2018.05.008](https://doi.org/10.1016/j.euromechsol.2018.05.008).
- [17] Y.Q. Wang, C. Liang, J.W. Zu. Examining wave propagation characteristics in metal foam beams: Euler-Bernoulli and Timoshenko models. *Journal of the Brazilian Society of Mechanical Sciences and Engineering*, 40(12):565, 2018. doi: [10.1007/s40430-018-1491-z](https://doi.org/10.1007/s40430-018-1491-z).
- [18] J. Wang, T.P. Morris, R. Bihanta, and Y.-C. Pan. Numerical and experimental verification of impact response of laminated composite structure. *Archive of Mechanical Engineering*, 67(2):127–147, 2020. doi: [10.24425/ame.2020.131687](https://doi.org/10.24425/ame.2020.131687).
- [19] A. Garg, and H.D. Chalak. Novel higher-order zigzag theory for analysis of laminated sandwich beams. *Journal of Materials: Design and Applications*, 235(1):176–194, 2021. doi: [10.1177/1464420720957045](https://doi.org/10.1177/1464420720957045).
- [20] K. Magnucki, E. Magnucka-Blandzi, and L. Wittenbeck. Three models of a sandwich beam: Bending, buckling and free vibration. *Engineering Transactions*, 70(2):97–122, 2022. doi: [10.24423/EngTrans.1416.20220331](https://doi.org/10.24423/EngTrans.1416.20220331).
- [21] K. Magnucki. An individual shear deformation theory of beams with consideration of the Zhuravsky shear stress formula. In *Current Perspectives and New Directions in Mechanics, Modelling and Design of Structural Systems*, Zingoni (ed.) pages 682–689, CRC Press, Taylor & Francis Group, Boca Raton, London, New York, 2022, doi: [10.1201/9781003348443-112](https://doi.org/10.1201/9781003348443-112).
- [22] K. Magnucki, and E. Magnucka-Blandzi. A refined shear deformation theory of an asymmetric sandwich beam with porous core: linear bending problem. *Applied Mathematical Modelling*, 124:624–638, 2023. doi: [10.1016/j.apm.2023.08.025](https://doi.org/10.1016/j.apm.2023.08.025).